Ultramicroscopy 25 (1988) 41–46
North-Holland, Amsterdam

THE USE OF DIGITAL SIDE-BAND IMAGE PROCESSING TO PRODUCE TOPOGRAPHIC CONTRAST

J.G. PÉREZ-RAMÍREZ, A. GÓMEZ, V. CASTAÑO and M. JOSÉ-YACAMÁN

Instituto de Física, UNAM, Apdo. Postal 20-364, México, DF 01000, Mexico

Received 2 October 1987

It is shown that by the use of image processing techniques, side-band topographic images of the type described by Cullis and Maher [Ultramicroscopy 1 (1975) 97] can be obtained. A displaced "electronic filter" is used on the Fourier transform of the image to introduce the contrast. The final reconstructed image shows characteristics similar to those obtained in the TEM with displaced apertures.

1. Introduction

In many characterization studies using TEM it is often necessary to increase the contrast of a particular feature in a situation in which the image has already been obtained, or to obtain additional information on a given region that was not considered when the experiment was performed. In these cases digital image processing can be used to obtain some additional information on the picture without the need for new experimental data.

It is well known in the literature that side-band images [1–4] are useful in obtaining topographic contrast of rough surfaces. This method has been used to determine small-particle sizes in supported catalysis [5]. The method consists basically of forming images in the bright-field mode using a semi-infinite displaced aperture. In the resulting images the contrast will depend on the incidence angle of the electron beam with respect to the normal to the surface. Thus topographic roughness on the sample will be enhanced in the image. In the present paper we will show that a similar effect can be obtained by digital image processing.

2. Example of side-band images

In order to illustrate the method let us consider the image in fig. 1, which corresponds to a gold particle with decahedral shape [6]. This particle contains three twin boundaries which are seen with very poor contrast. The image was digitized from a positive print using a standard TV camera and from the negative plate using a scanning microdensitometer. The data were then transferred to a VAX-1178 computer and the digital Fast Fourier Transform (FFT) was obtained. The display of the FFT is shown in fig. 1b. Then a digital aperture was introduced in the Fourier space to simulate the displaced aperture (as shown in fig. 1b). This procedure was done on an Innovion system for image display. The image was then reconstructed by a further Fourier transform. The result is shown in fig. 1c. The twin boundaries between the decahedral grains are now clearly observed, since their contrast has increased. Moreover, the observed contrast appears to be consistent with the idea that the boundaries are not flat but correspond to "notches" [7] produced in a

0304-3991/88/$03.50

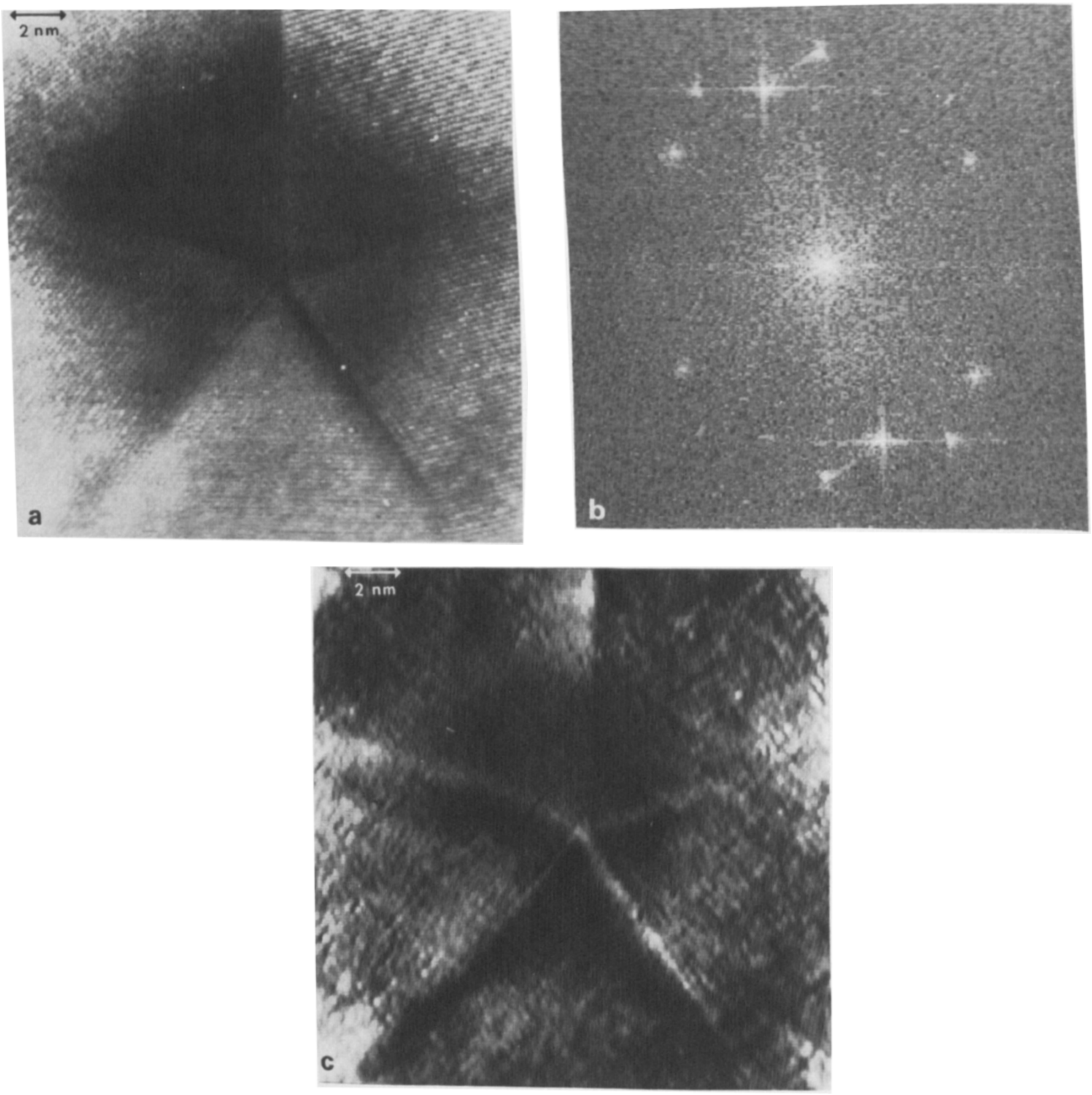

Fig. 1. Image of a gold particle with decahedral shape: (a) the conventional image; (b) Fourier transform of (a) showing the filter used to produce the image; (c) digital topographic image obtained by a displaced filter (see text).

large particle to relieve the stresses on the particle. This is in agreement with the data obtained using high resolution images [8]. In the next section we will discuss the theoretical aspects of this type of image.

3. Theoretical considerations

3.1. General considerations

Let $I(x)$ be the photographic density on the plate. In the following, only one dimension will be considered, the extention to higher dimensions being immediate.

Let $\hat{I}(t)$ be the Fourier transform of $I(x)$. The aperture function will be given by a step function

$$S(t)=\begin{cases}1 & \text{for } t\le 0,\\ 0 & \text{otherwise}\end{cases} \tag{1}$$

Since $S(t)=\frac{1}{2}[1+\mathrm{Sgn}(t)]$, where Sgn is the signum function,

$$\mathrm{Sgn}(t)=\begin{cases}1 & \text{for } t\ge 0,\\ -1 & \text{for } t\le 0,\end{cases} \tag{2}$$

the reciprocal space amplitude after the aperture is given by

$$\hat{I}'(t)=\hat{I}(t)\ S(t)=I(t)\frac{1+\mathrm{Sgn}(t)}{2} = \frac{I(t)}{2}+\frac{I(t)\ \mathrm{Sgn}(t)}{2}. \tag{3}$$

Now, since

$$\mathrm{Sgn}(t)=t/|t|,$$

and using the well known theorem in Fourier theory stating that

$$F(\mathrm{d}I/\mathrm{d}x)=2\pi \mathrm{i} tI \tag{4}$$

(here F denotes the Fourier transform operation), we obtain

$$\hat{I}'(t)=\frac{I(t)}{2}+\frac{F(\mathrm{d}I/\mathrm{d}x)}{2(2\pi\mathrm{i}|t|)}. \tag{5}$$

The second term indicates that part of the observed intensity can be regarded as a combination of a low-pass filter with a derivative.

If $I'(x)$ is the inverse transform of $\hat{I}'(t)$, then one usually calculates

$$|I'(x)|^2$$

which, by the previous equation, should resemble $I(x)^2+(\mathrm{d}I/\mathrm{d}x)^2$.

Note that the preceding equations are not well defined for $t=0$; this constitutes the "background" ambiguity discussed by Saxton and others [2].

The procedure involves, after all, a Hilbert transform as shown below.

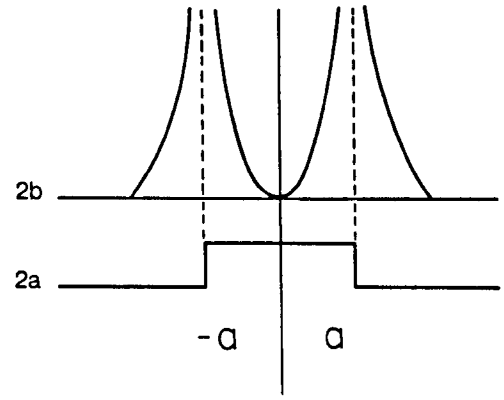

Fig. 2. (a) Schematic representation of a small particle of size a. (b) Processed image showing an enhancement of the contrast of the edges.

3.2. A particular case

Consider a "particle" with

$$I(x)=R(x), \tag{6}$$

where

$$R(x)\begin{cases}1 & \text{for } |x|\le a,\\ 0 & \text{otherwise,}\end{cases}$$

as shown in fig. 2a. Then

$$I(t)=F[R(x)]=\mathrm{sinc}(at). \tag{7}$$

Proceeding as in the previous section,

$$I'(t)=I(t)\ S(t).$$

Thus,

$$I'(x)=R(x)*S(x),$$

where

$$S(x)=\int_{-\infty}^{\infty}S(t)\ \mathrm{e}^{2\pi \mathrm{i}tx}\,\mathrm{d}t = \int_{-\infty}^{0}\mathrm{e}^{2\pi\mathrm{i}tx}\,\mathrm{d}t=\frac{-1}{2\pi\mathrm{i}x}, \tag{8}$$

$$R(x)*S(x)=\frac{-1}{2\pi\mathrm{i}x}\int_{-\infty}^{\infty}\frac{R(x-x')}{x'}\mathrm{d}x' = \frac{-1}{2\pi\mathrm{i}x}\int_{x-a}^{x+a}\frac{\mathrm{d}x'}{x'} = \frac{\mathrm{i}}{2\pi x}\ln\left|\frac{x+a}{x-a}\right|. \tag{9}$$

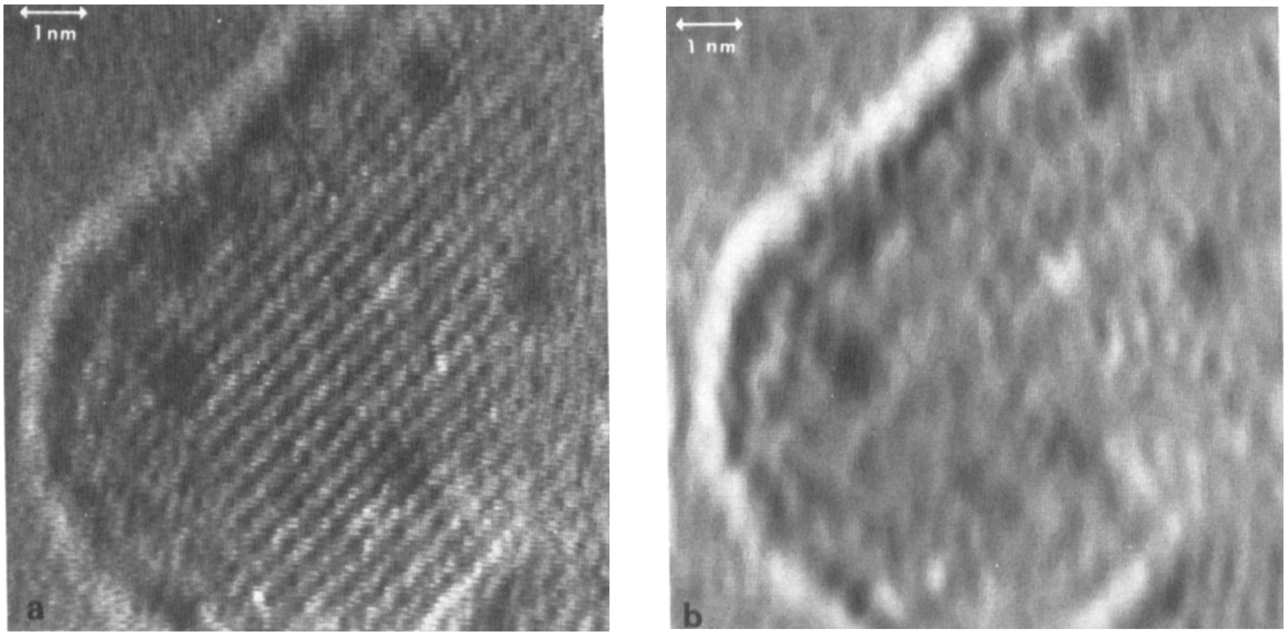

Fig. 3. Images of Rh/TiO_2 catalyst: (a) conventional image; (b) digital side-band topographic image.

Finally,

$$I'(x)^2 = \ln\left|\frac{x+a}{x-a}\right|^2. \quad (10)$$

A plot of eq. (10) is shown in fig. 2b which illustrates how the contrast of the edges is increased.

4. Applications to small particle studies

The technique discussed in the previous sections is particularly interesting for studying small metallic particles in supported catalysts. Fig. 3a shows a high resolution picture of Rh particles supported on a TiO_2 substrate [9]. Lattice fringes from the support can be observed. This type of picture does not allow a precise determination of the particle size. Fig. 3b shows the side-band image obtained after digital processing. The particles are now clearly distinguished and their size can be easily measured. In cases in which the particle contrast is particularly difficult to observe, such as in catalysts supported on $\gamma - Al_2O_3$, the present method gives some advantages over conventional pictures. In addition, in some materials it is not possible to obtain the topographic "electro-optical" images, therefore digital image processing becomes a very good possibility to obtain this extra information.

Since most of the features of the standard side-band images are obtained in this type of processing we can also conclude that:
- With this technique features can be observed which would be otherwise quite invisible (for example metal particles).
- It is possible to distinguish between hills and valleys using different displacements of the electronic aperture as suggested by Cullis and Maher [1].
- The distance between the black and dark contrast of an image gives the true size and shape of particles.
- The technique can reveal surface steps in the sample.

Acknowledgements

The authors are indebted to Mr. Samuel Tehuacanero for technical support in image processing and to Dr. S. Fuentes for providing the samples used in this work.

References

[1] A.G. Cullis and D.M. Maher, Ultramicroscopy 1 (1975) 97.
[2] W.O. Saxton, Computer Techniques for Image Processing in Electron Microscopy, Advances in Electronics and Electron Physics, Suppl. 10 (Academic Press, New York, 1978).
[3] S.G. Lipson and H. Lipson, Optical Physics (Cambridge University Press, 1969)
[4] W.O. Saxton, J. Phys. D7 (1974) L63.
[5] A. Gómez, P. Hernández and M. José-Yacamán, Surface Interface Anal. 4 (1982) 3.
[6] K. Heinemann, M. José-Yacamán, C. Yang and H. Poppa, J. Crystal Growth 47 (1979) 709.
[7] L.D. Marks and A. Howie, Phil. Mag. A49 (1984) 95.
[8] L.D. Marks, J. Crystal Growth 61 (1983) 556.
[9] S. Fuentes, A. Vázquez, J.G. Pérez-Ramírez and M. José-Yacamán, J. Catalysis 99 (1986) 492.